Original implementation of low-temperature SPS for bioactive glass used as a bone biomaterial

A Gharbi, S Ayadi, N Jouini, F Schoenstein, Hassane Oudadesse, H El Feki, W Cheikhrouhou-Koubaa

Original Implementation of low-temperature SPS for bioactive glass used as a bone biomaterial

A. Gharbi[a,b], S. Ayadi[c], N. Jouini[c], F. Schoenstein[c,d] H. Oudadess[b], H.el Feki[a]

W. Cheikhrouhou-Koubaa[a]

[a]*Sfax University, Faculty of Sciences of Sfax, 3018 Sfax-Tunisia*
University of Rennes 1, ISCR, UMR CNRS 6226, 35042 Rennes- France
[c]*University of Paris 13, LSPM, CNRS-UPR 9001, 93430 Villetaneuse- France.*
[d]*University of Paris Est, ICM, CNRS-UPEC-UMR7182, 94320 Thiais-France.*

ABSTRACT

Alkali borated bioactive glasses powders with compositions based on the SiO_2-Na_2O-CaO-P_2O_5-x B_2O_3 system (0 <x< 20 wt.%); have been consolidated at low temperature using Spark Plasma Sintering (SPS). Through SPS technique under 50 MPa, it was possible to achieve fully dense and completely amorphous borated glasses at temperatures as low as 420°C. By increasing the sintering temperature up to 430°C, the dense samples crystallized which is mostly achieved at higher temperatures. This study reveals that the mechanical properties of these new borated biomaterials are suitable to be used as a promising candidate for repairing defects in non-load-bearing bones as well as for coating on the metallic surface implants to improve the bioactivity process bone/implant. The pressure had a weak effect on the crystallization and densification of the glass compared to the temperature during the powder consolidation by SPS. Moreover, by increasing the boron content, the compressive strength and the elastic modulus of the elaborated glasses decreased for being close to those of the natural.

Keywords: Borated bioactive glasses; Spark Plasma Sintering; mechanical behaviour.

1. Introduction

Traumatic calamities and diseases frequently cause difficult damages to the musculoskeletal system; even more, the ageing of the population is likely to result in more and more diffused

bone tissue disabilities. To overcome such problems, the expansion development and optimization of innovative synthetic bone graft substitutes such as bioactive glasses (BG) are becoming an urgent need [1,2].

Bioactive ceramics and glasses have been used for decades in the surgical repair of injured bone and teeth due to their biocompatibility and advantageous physical and mechanical properties that are close to those of 'hard' tissues [3].

These materials and mainly those based on Silicon (Si) show a high bioactivity index and a perfect ability to bond with both hard and soft tissues [4]. Recent research has even been interested in the development of multifunctional nanoparticles, consisting of binary bioactive glass (SiO_2-CaO), for local cancer treatment by magnetic hyperthermia and bone regeneration [5]. It has been shown that amorphous BG can react with physiological fluids forming persistent bonds to bone across the formation of bone-like hydroxyapatite (HA) layers leading to biological fixation of bone tissue with the glass surface [6, 3].

Recently any studies improve this biocompatibility by adding some chemical elements such as boron (B) which presented interesting physiological properties. The introduction of boron in the glass network of the CaO-B_2O_3-P_2O_5 system had a catalytic effect on favouring the bioactivity of the other calcium phosphate glasses [7]. Adding boron to 45S5 Bioglass®, ameliorates the rate of HA formation on the surface of the glass. As a result, the glass showed an increase in cellular bioactive behaviour [8,9].

On the structural hand, the studies showed that doping with B_2O_3 promotes glass powder densification with similar chemical compositions [10]. It is well known that crystallization, biological and mechanical behaviours of bioactive glass are importantly related by the relative amounts of the different oxide constituents [11].

The originality of this work is the understanding of the effect of silicon (Si) substitution by boron (B) on the mechanical proprieties of these materials so that they can be adapted to different orthopaedics 'needs. Among the specific criteria for ideal BG used in bone tissue engineering is the ability to deliver cells, excellent osteoconductivity, good biodegradability, suitable microstructure, and appropriate mechanical properties [12,13]. This biomaterial type has proven to have high biological performance when embedded in cranial implants [14]. Moreover, the available research results show an improvement in the mechanical properties of

bioactive glass-ceramic scaffolds as a result of recent research efforts, making it possible to consider the use of bioactive glass-ceramic scaffolds in clinical applications [15].

An evaluation of the structural and mechanical properties of aerosol deposited bioceramic films for orthodontic brackets was proven using HA-brushite and SiO_2-Al_2O_3 biocompatible nanostructured coating layers. The obtained samples led to high-performance orthodontic brackets, such as a successful clinic and improved bond strength [16]. Furthermore, hydroxyapatite (HA) bioceramic composites fabricated using digital light processing (DLP) showed excellent mechanical properties and degradation behaviour [17]. In order to improve the mechanical dependability of biomedical glass, several approaches have been suggested, such as the production of sintered bodies.

Bioactive glass 45S5 is well known for its poor sintering behaviour due to the inhibition of viscous flow by the crystallisation of the sodium and calcium silicate phases. New research demonstrates that sintering can be significantly improved by the partial or complete substitution of (Mg) or (Zn) [18]. However, an issue related to the sintering of bioactive glass powder is its tendency to rapidly crystallize above the glass transition temperature (Tg). Hence this thermal character prevents the full densification and this is the case of 45S5 Bioglass® powder [19].
Thereby the pressureless sintered models obtained at temperatures below 600°C, present a low mechanical strength [20]. This is a pertinent drawback since crystallization is a way to decrease the bioactivity of the glass [21,22].
As well under pressureless sintering conditions, BG-45S5, like other bioactive glasses possess a rapid crystallization already at ~580–650 °C, leading to a practically totally crystallized solid at low temperature before the full densification [16,23]. Other papers find that the first crystallized phase in bioactive glass BG-45S5 appears between 600 and 700°C and around 800°C, they discovered the crystallisation of a second phosphate phase. After the glass transition and before crystallisation, a spinodal separation of glassy phases into two immiscible phases appears, one rich in silica and the other rich in phosphorus [24]. Thus, it is impossible to obtain amorphous and fully dense models through a conventional sintering route. Hence a non-conventional technique was proposed in this paper.

The spark plasma sintering (SPS), was used to consolidate the borated glasses powders at non-conventional, very low temperatures (T< 450°C) to preserve the amorphous character and to achieve full densification. As a result, we may obtain samples that exhibit high densification,

good mechanical properties and an intact amorphous structure. The sintering route using SPS offers an established technological and economical approach for the manufacture of orthopaedic implants [25,26]. In this regard, the research describes the simultaneous improvement of mechanical and biological properties of silicate-based Hydroxyapatite by incorporating hybrid nanosheets S-rGO prepared by SPS [27].

It is evident that to allow the ingrowth of new bone tissue, good vascularization, and the firm fixation of the implants, it is necessary to control the elastic limit and Young's modulus in order to improve the biomechanical compatibility of the implants. For example, the alloys used for orthopaedic implants have Young's modulus in the range of 55–80 GPa (depending on sintering temperature [28]). This large disparity of elastic modulus between the implant materials and the human bones (1–2 GPa for cancellous bones and 2–20 GPa for compact bones [3]) may lead to the resorption of the human bone, loosening of the implants and finally, the failure of implantation [29,30].

In this paper, we investigated the sintering behaviour of a new B_2O_3-subsisting SiO_2-Na_2O-CaO-P_2O_5 system (BG-B_x) previously prepared by the melting process where x is the amount of B_2O_3[31]. The sintering route offers a well-established technological and economical approach for manufacturing net-shaped bioactive glass materials. After understanding the mechanical and thermal proprieties of the borated glasses, we could suit these materials to the different orthopaedic needs.

2. Experimental procedure

The introduction of boron (B) into the silicate glass structure of resorbable bioactive glasses represents a scientific revolution. Because of its valuable chemical and optical properties, the boron-based amorphous network configuration can be favourable to move toward fully resorbable biomaterials-based sensors or bone substitute agents, to avoid additional surgical procedures for the patient to remove the implant after use [32]. For these special needs, we will join these new features by the development of a new bioactive/bioresorbable boron derivative. Borated bioactive glass (BG-B_x) powders with an average particle size of 40 μm were used as the starting materials. The advanced chemical composition of these glasses, and their amounts at the beginning of the experiment, in wt%, are listed in Table 1.

The consolidation process of powders was realized by a spark plasma sintering (SPS)-515S SYNTEX apparatus. This device consists of a uniaxial press with a maximum force of 200 kN and a power supply able of producing a pulsed DC current with a maximum of 8000 A at 10 V. Glass powder samples (1g) were placed in a 10 mm graphite die. Thin graphite sheets (Papyex) were used between the powder and the die to facilitate the removal of the sintered sample. The filled die was then introduced in the treatment chamber under low mechanical pressure in order to ensure electrical contact of the system. The treatment chamber was purged twice under vacuum and then 1 atm argon pressure was applied during the sintering/consolidation process. The SPS samples were sintered at a temperature of 420 °C. In order to obtain amorphous and dense samples, the sintering temperature was set below the crystallization temperature (≤ 510 °C [33]) while the pressure was fixed at 50 MPa. In all of the SPS tests, the temperature was controlled by a type K thermocouple, and the heating rate was 50 °C/min. The uncertainty in the temperature measurement was underneath 5°C. Just before the sintering temperature, the heating rate was reduced to 10 °C/min to avert glass crystallization risk. Thus, relatively high heating rates might correspond to higher sintering temperature due to the inhomogeneous temperature distribution. Similarly, low sintering temperatures are recommendable to limit carbon contamination due to the SPS graphite dies. Moreover, the holding time was 2 min at the sintering temperature. After the SPS process, the experimental density was determined with a pycnometer (ULTRAPYC 1200 to helium displacement (He)) at room temperature with an accuracy of 0.002 g/cm^3. Each value is an average of two independent measurements and then averaged to obtain reliable results. The error on density measurement is assumed below 0,01%. Then, the relative density values were calculated assuming 2.7 g/cm^3 as the theoretical density of the Bioglass® 45S5 [34]. Further, The XRD patterns of sintered glasses were obtained using a (θ–2θ) Panalytical XPERT PRO MPD diffractometer operating with Cu Kα radiation. This characterization was realised to prove the amorphous character stabilization of the post SPS cylinder. Besides, the morphology was studied by scanning electron microscopy using FEI Quanta 200 environmental scanning electron microscope. The synthesized surfaces were covered by a gold-palladium layer (Au - 20 wt. % Pd) to allow surface conduction. The samples were cut using a diamond saw. Using a traction machine of type 10 kN MTS the compressive strength tests at a cross-head speed of 1.0 mm/min were carried out on the various biomaterials (Fig. 1). The samples were placed between the plates of the testing machine. The force-displacement curve was analyzed with Nexygen 4.0 software.

The Young's modulus was obtained by an ultrasonic technique using an Olympus apparatus.

3. Results and discussions

3.1. Densification of bioactive glasses (BG-B_x):

A brittle material that lacks fracture toughness is not appropriate for use in bone-defect grafting or bone-tissue engineering. For this latter goal, the densification process to improve the mechanical properties has been tailored by the sophisticated sintering technique of SPS for all the bioactive glass specimens. The temperature and pressure programmed sequences are described in Fig. 2.

A defect-free vitreous material does not include a second crystallized phase. Nevertheless, all glasses crystallize but at different rates in the temperature range between its characteristics temperatures [35,36]. In order to obtain a homogeneous temperature distribution inside the sintering sample, a slow heating rate (50°C) was performed to promote densification at a lower temperature (420°C). It is well known that SPS process in lower sintering temperatures as well as shorter sintering cycles [37] compared to conventional sintering CS and hot press techniques. Newly proven, the better mechanical strength, fatigue strength, higher density, finer grain structures, higher hardness and superior tissue growth in cell culture have been stated with alumina-zirconia bioceramic composites processed via spark plasma sintering as compared to conventional processes [38]. In that sense, Kanhed and al. [34] observed that microwave-sintered porous HA presented improved mechanical properties, i.e., fracture toughness (7.5 MPa) and hardness (183.7 VHN). These samples are able to successfully arrest the crack and offer maximum resistance to its propagation due to their rapid heating rate (100°C/min), compared to that of CS (5°C/min) [39]. Characteristically, high heating rates for electrically insulating materials result in non-homogeneous temperature distribution inside the sintering sample due to the poor thermal conductivity of the green compact [40]. As shown in Fig. 2 the powder densification is obtained essentially when the temperature and the pressure achieve the bearing. Thereby, the further information from these plots of shrinkage and temperature profile is that the boron addition into the vitreous network slows down the densification process of bioactive glass when it is consolidated by SPS. Thus, the densification durations (in "minute:

second") which correspond to the fully amorphous borated glasses were illustrated in the following Table 2.

The samples added with different amounts of B_2O_3 in mass% present a nearby relative density. Moreover, these values increase from 98,76% to 98,93%. Such results indicate that B_2O_3 addition induces the bioactive glass disc to be more tightly pressed, consequently leading to an increase in relative density. When the sintering temperature was below Tg, high pressure favours the powders compaction. To reach amorphous materials with a density higher than 98% a sintering pressure of 50 MPa was needed at 420°C. On the other hand, the densification of the 45S5 Bioglass® (45 wt.% SiO_2, 25 wt.% Na_2O, 25 wt.%, CaO and 5 wt.% P_2O_5) powder in the temperature 350 °C was investigated under applied pressures of 70 MPa [23]. Bretcanu and al. [41] mentioned that the glass transition temperature of the Bioglass® 45S5 for heating rates between 5 and 30°C/min varies in the range 500–550°C. Likewise, Guillon et al. [42], using a slow heating rate (20 °C/min) achieved dense materials within 2 h under low compressive stress (0.5 MPa) at a temperature of 610 °C. Another advantage of low-temperature SPS sintering is the precise control of bioactive glass crystallization [36]. Most existing literature on the sintering of 45S5 Bioglass® shows that thermal treatments above 600°C result in the formation of the $Na_2Ca_2Si_3O_9$ phase as the main crystalline phase. ~~As reported by Lefebvre and al. [17] the crystallization of 45S5 Bioglass® depends on glass particle size and heating conditions.~~ More exactly, Bioglass® 45S5 forms crystalline $Na_2CaSi_2O_6$ when heated above 550-600°C [43], which is very near to its glass transition temperature, so crystallisation is practically inevitable during sintering [44]. The presence of crystalline phases can significantly slow the formation rate of nanocrystalline hydroxyapatite on the material surface; nevertheless, it has been reported that the 45S5 composition retains low bioactivity even after reaching 100% of crystallinity [45,46]. In the present study fixing the sintering temperature at 420°C, 50 MPa of pressure was enough to achieve borate bioactive glasses (particle size < 40µm) with a density exceeding 98%. The typically polished powder discs of 10 mm in diameter, and 5 mm in thickness are shown in Fig.3:

After SPS, samples of different relative densities (from 98,76% to 98.93%) were obtained for different B_2O_3 added amounts into the vitreous matrix of glass. Figure 3 exhibits the colour of SPS samples, having different relative densities. It has also to be underlined that the fully dense dark sample, D = 98.93%, corresponds to the BG-B_{20} glass. Since scrupulous "under-

stoichiometry" does not exist in amorphous glasses (no periodic lattice enabling lattice point defects formation), the colour change is possibly due to graphite ~~contamination~~ residue of the samples [47]. Furthermore, observation of graphite particles by SEM microscopy proved this point. The amorphous phase of the as-sintered powder disc was proved by XRD. Fig. 4 shows the XRD profiles of the powder sintered discs with 0, 5, 10 and 20 mass% B_2O_3 additions into the vitreous network of bioactive glasses. The XRD pattern exhibits the standard behaviour related to a vitreous material. All samples were in the amorphous phase since just a weak wide-spreading band has been recorded and no distinguishable diffraction peaks of crystalline phases in each XRD profile, confirming the fact that no crystallization at all occurred during the SPS sintering experiments for all BG-Bx glasses. A similar XRD pattern was also observed in another study, in which nano 58S BG powder had been elaborated through a specific sol-gel method [48]. XRD patterns of calcium silicates have diffraction with a board and asymmetric maxima at 2θ=32.0 [49,50]. The amorphous calcium silicate phase within the glass network of bioactive glasses may start to be crystallised at a temperature of about 800°C or above [51]. However, similar peaks have been observed even at a lower temperature in a study realized by Meiszterics and al. [52]. In addition to high temperatures, progressive cooling in the melting process for glass synthesis, as adapted in this research, or re-heating of elaborated glasses to the temperature below their melting temperature, were specified in literature as reasons for glasses crystallization [53].

To further confirm the microstructures of the sintered glass discs, the fracture surface and the surface appearance were observed by SEM, as shown in Fig. 5. and Fig. 6. respectively.

As confirmed by XRD, no crystalline phase forms at the sintering temperature of 420 °C. Some gaps were apparent on the fracture surface, as shown in Fig. 5. In addition, these last SEM observations of the polished surfaces are characterised by a dense and well-filled texture, especially for those that are doped with boron. These results are in coherence with those recently published by Leonie and al. who found that boron incorporation increases the surface bulk modulus of the mesoporous bioactive glasses with the molar composition of 80 % SiO_2–15% CaO–5% P_2O_5– (0.5–15%) B_2O_3 [54]. Moreover, some spaces in the powders, corresponding probably to the graphite particles, were evident on the polished surface, as shown in Fig.6 at the level of red allows, which indicates that the glass disc contains some defects. By observing the fracture surface, it is still possible to detect the amorphous morphology of the particles, even after sintering. ~~Comparably, as proved by Salvatore and al. [23], the fabrication of dense 45S5~~

~~Bioglass® compacts at low temperature (≤ Tg) is an interesting result notably for the fabrication of tolerant Bioglass® based composites where the Bioglass® matrix remains amorphous~~. The absence of viscous flow which is generally associated with sintering above Tg is evidenced by the untightened cohesion of the starting glass particles (Fig. 5). Thus, the presence of pores at even higher magnification is compatible with the material being microporous. The borated bioactive glass densities are very close to the density of human bone (1,8– 2,1 g/cm^3) [55]. In recapitulation, the SPS technique performed with accurate control of the processing parameters has allowed the production of dense and amorphous borate bioactive glass compacts which are expected to have improved bioactive response. ~~On the other side, as proved by Lefebvre and al. [17], by employing the Scherrer equation at the strongest intensity peak, the SPS sample sintered at 600 °C resulted in the formation of very fine $Na_2CaSi_2O_6$ crystallites with particles of about 25 nm immersed in an amorphous matrix of Bioglass® [37].~~ Moreover, we resonated that the relatively low density of the weak-boron amount discs (BG-B_0, BG-B_5) could be caused by the formation of a SiO_2 insulator layer coating that inhibited the discs from being tightly compressed as well as reduced eddy current. Similarly, Xue Li et al. [56] confirmed the formation of the SiO_2 insulator layer coating on an SiO_2-$Fe_{76}Si_{9,6}B_{8,4}P_6$ amorphous discs after sintering by spark plasma sintering technique.

This compaction success has been, according to several works, ensured by technological innovations in the field of SPS consolidation [57, 58, 59]. Besides, the chemical composition of the starting material, the sintering temperature and the pressure has an important role in the final material's morphology. Therefore, the BG-B_X glasses consolidated by SPS sintering have suitable densities and microstructures to become a promising candidate for the cortical bone implant. On the other side, the microstructure dependence of elastic and shear moduli in 45S5 glass-derived is well described by many mathematical models (Gibson, Arnold, Roberts and Nie model) across a fairly wide range of porosity around 40-85% vol. typical of human cancellous bone and, therefore, is recommended for biomedical substitutions [60].

3.2. Mechanical properties of bioactive glasses (BG-B_x):

Bioactive glasses are by nature brittle and lack fracture toughness. The most critical property that a biomaterial must possess is the ability to support mechanical loads, without excessive bending, permanent deformations, or early failures [61]. To be able to say about mechanical properties, it is first important to explain some basic definitions. Among the most important

mechanical properties of a biomaterial can be assessed by compression tests. The stress-strain curve can be obtained from these tests. The stress (σ) is defined as the force (F) per cross-sectional area (A0) (Eq.1), while the strain (ε) is set as the length change (Δl) of the sample scaled by its original length (l) (Eq.2) [62].

$$\sigma = \frac{F}{A_0} \quad (\mathrm{N/m^2 = Pa}) \tag{1}$$

$$\varepsilon = \frac{\Delta l}{l_0} \tag{2}$$

In this paper, the stress-strain curves presented are compatible with those of the brittle materials, which show that, after a certain stress value (σ), the material reaches its elastic limit i.e. its maximum resistance (R_{max}). At this limit point, the atoms are rearranged in different ways. For brittle materials and after reaching the limit or rupture point, the atoms separate from these bonds, which lead to "breaking" the glass. In addition, increasing the P_2O_5 content results in a decrease in compressive strength [63]. The operating conditions used are those adapted by H. Yli-Urpolors, who worked on bioactive glass in the 53% SiO_2-23% Na_2O-20% CaO- 4% P_2O_5 system [64]. The compressive stress-strain curves of the borated bioactive glasses with different relative densities are shown in Fig. 7 (after corrections and by ignoring the procedure error).

Unlike elastic materials, bioactive glass presents peak stress (σ) considered as the compressive strength of the sample, where the rupture of samples has occurred after a linear elastic deformation region [65]. All samples follow an elastic behaviour with small length change, that is to say, of ordinary deformations less than 0,012; i.e., 1,2%. Besides, the samples are ruptured in the linear part of the elastic zone. Therefore, the determination of the exact elastic limit value is difficult especially with a very low length change (<1%). For this, only the maximum stress (σ) evolution (mechanical strength) will be discussed. The experimental values are shown in Table 3.

By increasing the boron quantities into the vitreous network, the compressive strengths of borated discs decreased from 33MPa to 52MPa for samples with 20% wt. and 5% wt.,

respectively. The elastic limit values of glasses were close to those of bioactive glasses earlier elaborated [59]. Although, the compressive strength of the BG-B_X which ranged from 33MPa to 58MPa was lower than the compressive strength of natural bone (100–230MPa for cortical bone and 2–12MPa for cancellous bone [3]). The evolution of the elastic limit (R_m) with the boron percentage is shown in Fig.8.

It could be seen that the maximum stress (σ) of the glass decreased by increasing the boron content in the glass. Thus, these mechanical strength values are higher than those stated by O. Prokopiev and I. Sevostianov [66], who worked on hydroxyapatite specimens, sintered using an electric furnace for 3 hours (the mechanical strength does not exceed 14MPa). Otherwise, these mechanical characteristics of the vitreous biomaterials are incomparable for the metallic biomaterials, such as Ti and Ti–6Al–4V alloy [67,68,69]. Other review reports that PCL/borosilicate glass hybrid biomaterials containing 50wt% trimethoxysilane functionalised polycaprolactone (PCL) and 50wt% boro-phospho-silicate (B_2O_3-P_2O_5-SiO_2) glass (BPSG) showed compressive strength, modulus and toughness values of 32.2±3.5 MPa, 573±85 MPa and 1.54±0.03 MPa, respectively [70]. After the compression test, SEM analysis manifests the fracture facies of BG-B_{20} sample (Fig.9.) in order to show the glass microstructural evolution during the elastic deformation. At 1.2% length change, these SEM images show the slip traces, at different magnifications. Indeed, it is clear that the surface is slightly scratched, indicating low internal friction within the glass during compression. This observation further proves that the boron addition into bioactive glasses reduces their mechanical strength.

In general, the compressive strength behaviour of the dense biomaterial mainly depends on the initial chemical composition and the heat-pressure treatment process. Moreover, with the combination of the relative density, SPS process, pure phase composition, mechanical properties, it could be concluded that the borated bioactive glass is capable to become a promising candidate for a bone implant. The schematic example of the stress-strain curve evaluated with a compression test on the brittle material BG-Bx shown in Figure 7 reveals other important data on the mechanical properties of this biomaterial type. In the major part of these curves (approximately up to 1% strain) the material behaves elastic, which means that the deformation is reversible. This linear region of the elastic behaviour is described by Hooke's law, which results in a material characteristic that is a function of the material stiffness: the Young's modulus or elastic modulus (E in Eq.3) [57].

(3)

The Young's modulus is another important mechanical property for the bone-implant materials besides the compressive strength. The elastic modulus (E) of the sintered bioactive glasses with different amounts in boron is shown in Fig. 10.

$$E = \frac{\sigma}{\varepsilon} \text{ (Pa)}$$

The Young's modulus of the sintered biomaterials almost linearly decreased from 56,3 GPa for the sample with boron amount of 5% to 27,1 GPa for the sample with 20% boron amount by increasing the boron added quantity into the glass matrix, all of which was higher or close to the elastic modulus of natural bone (3–20 GPa for cortical bone and 0,05–0,5 GPa for cancellous bone [3]). The elastic modulus values of the synthesized bioactive glasses are listed in Table 4.

The elastic modulus values of borated glasses are similar to those of hydroxyapatite sintered at 800 ° C under a pressure of 100MPa [71]. ~~On the other side, the obtained values are lower than those quoted by L. Desogus and al. who worked with the following molar composition: 2,3% Na_2O 2,3% K_2O 45,6% CaO 2,6% P_2O_5 47,2% SiO_2 [52].~~ Thus, the elastic modulus evolution as a function of the relative density is shown in Fig.11.

The decrease of elastic modulus with the increase of boron quantity introduced into the glass is very clear. Indeed, we can assume that the boron addition reduces the mechanical strength of bioactive glasses even after sintering. These mechanical behaviours can be explained by a brief structural analysis of borosilicate glasses. The glass network formers (M) are covalent compounds such as silicon (M=Si) and boron (M=B) oxides. They are readily vitrifiable elements. These oxides form a disordered sequence of a tetrahedron of 3 or 4 co-ordination linked at their apex with oxygen atoms or the M-O-M bond is an ion-covalent bond [72].

As illustrated in Fig. 12, in silicate glasses, the vitreous network is characterised by a three-dimensional geometry consisting of tetrahedrons type (SiO_4), linked together by bridging oxygens (≡Si-O-Si≡) [30].

From ^{11}B NMR measurements performed on borosilicate glasses of composition SiO_2, B_2O_3, Na_2O, a model has been proposed to suggest the coordination ratios of 3 (B^{III}) or 4 (B^{IV}) [73].

Further structural studies proved that boron ions in the silicate glass network participate with the structural units of form BO_4 and BO_3 with the dominance of the latter [74].
Indifference to the three-dimensional structure of the silicon network, the chemical entity forming the boron network has a plane spatial geometry as shown in Fig. 13. The BO_3 entities form planar triangles linked together at the apexes and form planar rings $(B_3O_6)^{3-}$ called boroxols (for 60-80% of the boron atoms). Although it is known that the boron atom lies just above the plane formed by the oxygen atoms of the triangle, the quasi-planarity of these entities makes $(B_2O_3)^{-}$ substituted glass much more brittle than a three-dimensional glass composed of the tetrahedron as in vitreous [75].

Due to their relatively low modulus of elasticity according to the added boron amount, their applications can be well adapted to non-load-bearing implants. However, bioactive glasses can be successfully implemented for coatings on the metallic surface implants to associate the adequate mechanical properties of metal alloys to bioactivity and biocompatibility of bioactive glasses [76]. For this study, by only considering the compressive strength and the elastic modulus, the borated bioactive glasses sintered by the SPS process could be a promising candidate for the hard tissue repair and replacement implant.

Conclusions, Challenges and Future Perspectives

In our view, the improvement of borosilicate network mechanical strength while retaining its physicochemical and optical properties is one of the major challenges for the development of bioactive glasses next generation. In this way, the choice of sintering technique is highly dependent on the nature of the bioactive glass and the specific nature of the biomedical device to be used, as different characteristics are required for each application. Furthermore, the SPS technique allows the use of a wide range of compositions of bioactive glasses that are not supported in conventional sintering, with the advantage of low-temperature treatment. From this point of view, it was possible to achieve fully dense and amorphous borate bioactive glasses with a sintering temperature as low as 420 °C. In agreement with this achievement, the elaborated biomaterials relative densities increased by adding boron oxide B_2O_3 into the vitreous matrix furthermore the corresponding maximum densification duration extended. According to our previous studies, B_2O_3 oxide is introduced in bioactive glass compositions, to decrease the crystallization temperature to improve cell proliferation during and after

implantations, and therefore to achieve bioactive glasses with low susceptibility to devitrification during thermal treatment. under these optimal conditions of synthesis and sintering, the consolidated boron-glass samples possess acceptable compressive strengths. Moreover, by increasing the boron quantity in the initial chemical composition, all of the elastic limits and Young's modulus of the borated discs decreased to conform with the requirements of non-load bearing human implants. However, this could be an important advancement of the current state-of-the-art to build also multi-functional bioactive coatings. The use of borated bioactive glass as an orthopaedic implant depends on several medical needs (patient age and sex, implantation site .....).

The growing need for the biomedical implant is leading research to investigate shaping techniques and optimise the parameters of biomaterial synthesis and sintering to assess which are optimal for filling, therapy or even detection requirements. However, the principal direction of investigations should be on the achievement of the greater comprehension of bioactive glass chemical compositions, as well as in terms of the influence of the added elements. Bioactive glasses can be produced with certain compositions able to enhance a specific response in the host or to introduce antibacterial properties. Bioactive glass compositions could be tailored depending on the specific deposition techniques adopted, to obtain well adherent coatings and to reduce failure. Bioactive glasses can be produced with selected chemical compositions that can enhance a specific response in the host or provide antibacterial properties. The bioactive glass initial compositions could be adapted according to the different medicinal applications, to ensure appropriate biological and mechanical adhesion. In this regard, bioactive glass presents a great advantage compared to ceramic surgical implantation, such as hydroxyapatite or calcium phosphates, because bioactive glass compositions can easily be adjusted.

Future work should be targeted on the study of the optimal combination of synthesis procedure, sintering parameters, and chemical compositions that could facilitate the optimisation of implant multifunctional uses. In order to promote human tissue healing and regeneration.

Finally, it is worth noting that the bioactivity of our glasses has been widely investigated by immersion in SBF solution. On the contrary, in vitro and in vivo tests on metallic implants coated by bioactive glasses are still limited. The investigation of glasses biocompatibility by in vitro tests and, more importantly, preclinical studies in animal models should be essentially increased. Furthermore, research on stability over time and long-term properties should be fundamental, because it permits one to investigate the response of implants once implanted in the human body, which is a complex and dynamic environment. This should be one of the most important goals for the future.

Acknowledgement:

This work has been supported by the Tunisian Ministry of Higher Education and Scientific Research.

Figure captions

Fig.1. Schematic diagram of the test samples in the compression experiment.

Fig.2. Schematic variations of temperature, displacement and pressure as a function of holding time SPS.

Fig.3. Evolution of the aspect versus the relative density for borated glasses sintered by SPS at 420°C, under 50MPa and during 2 min

Fig.4. XRD patterns of dense samples sintered by SPS (50°C/min – 420°C – 50 MPa – 2 min).

Fig.5. SEM micrographs of fracture surfaces of BG-B_X samples sintered at 420°C.

Fig.6. SEM images with relative densities indication for polished surfaces of BG-B_X.

Fig.7. Compressive stress–strain curves of the borated bioactive glasses: BG-B_X.

Fig.8. Elastic limit of biomaterials with various boron quantities added into the vitreous network. Vertical lines represent standard deviations.

Fig.9. Cross-sectional micrographs of BG-B_{20} sample after the compressive strength test.

Fig.10. Elastic modulus variations for the contents: 0, 5, 10 and 20%wt. in boron added in the glass.

Fig.11. Relationship between elastic modulus and relative density of borated bioactive glasses.

Fig.12. A single SiO_4 tetrahedron unit

Fig.13. Plane geometric structure of BO_3 unit

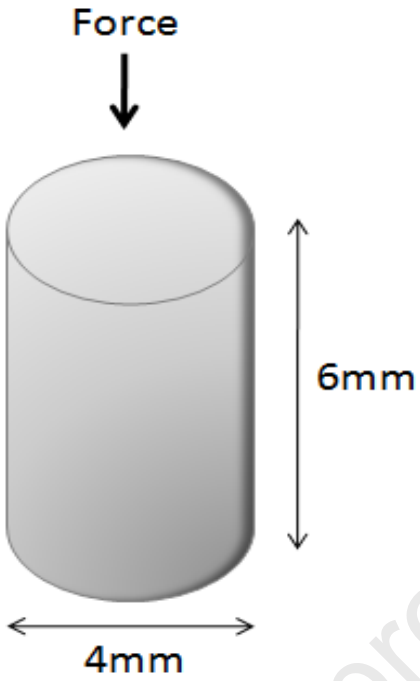

Fig. 1

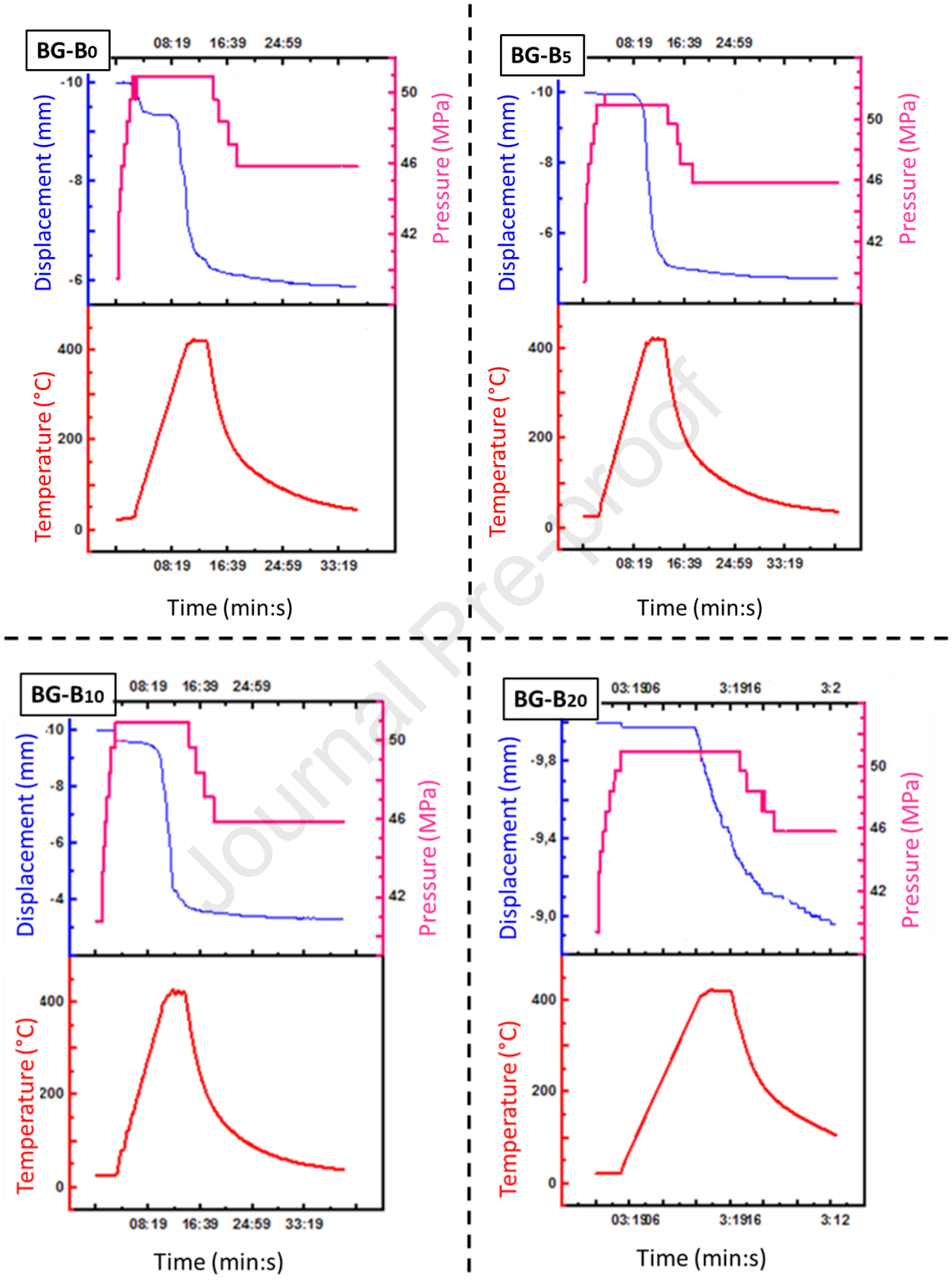
BG-B0
BG-B5
BG-B10
BG-B20
Displacement (mm)
Pressure (MPa)
Temperature (°C)
Time (min:s)
08:19
16:39
24:59
33:19

Fig. 2

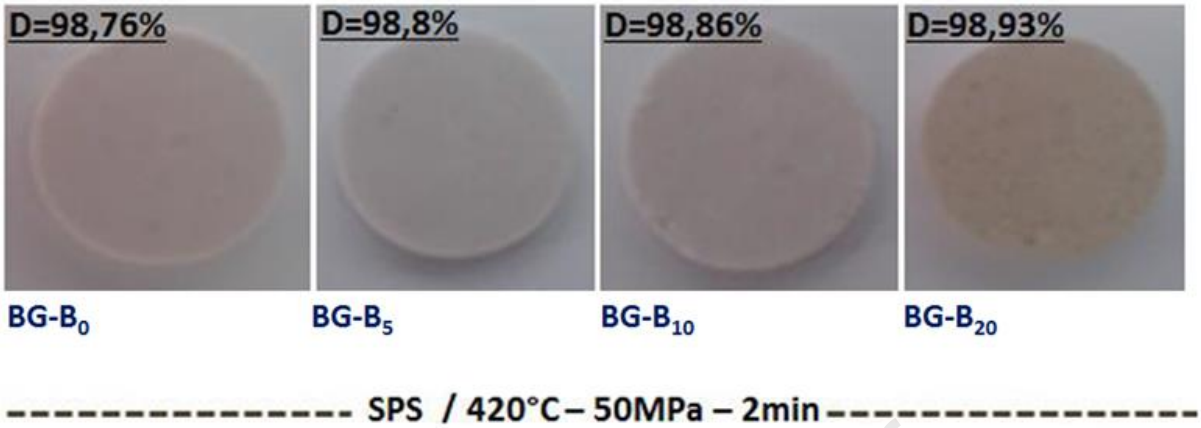
D=98,76%
D=98,8%
D=98,86%
D=98,93%
BG-B0
BG-B5
BG-B10
BG-B20
SPS / 420°C – 50MPa – 2min

Fig. 3

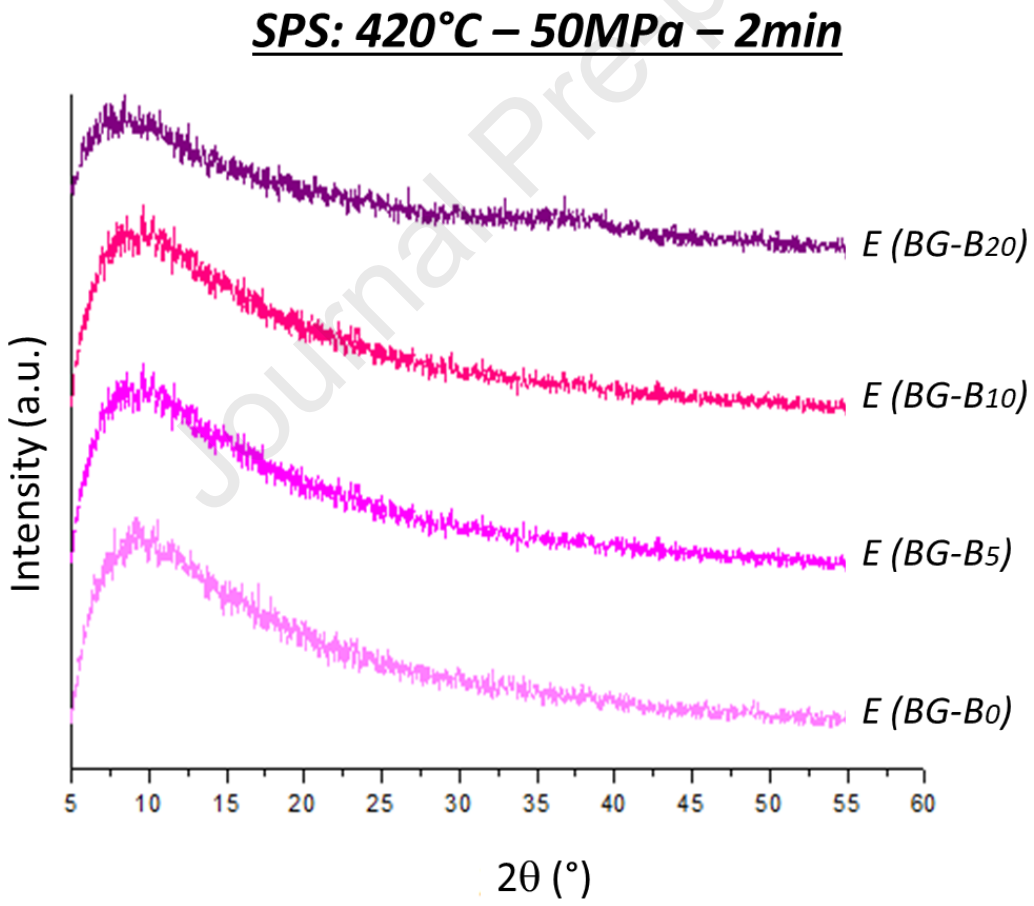
SPS: 420°C – 50MPa – 2min
Intensity (a.u.)
E (BG-B20)
E (BG-B10)
E (BG-B5)
E (BG-B0)
5
10
15
20
25
30
35
40
45
50
55
60
2θ (°)

Fig. 4

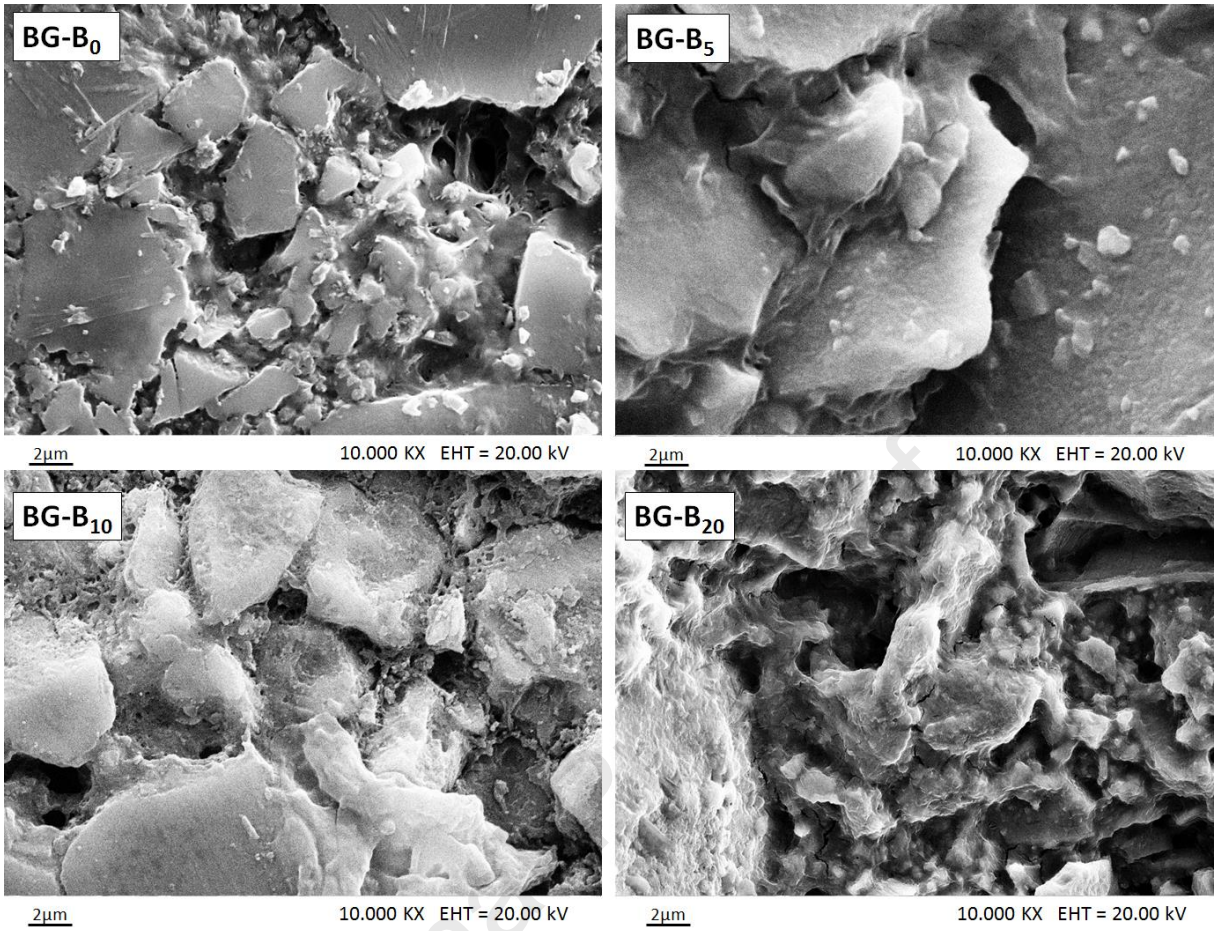
BG-B0
2µm
10.000 KX EHT = 20.00 kV
BG-B5
2µm
10.000 KX EHT = 20.00 kV
BG-B10
2µm
10.000 KX EHT = 20.00 kV
BG-B20
2µm
10.000 KX EHT = 20.00 kV

Fig. 5

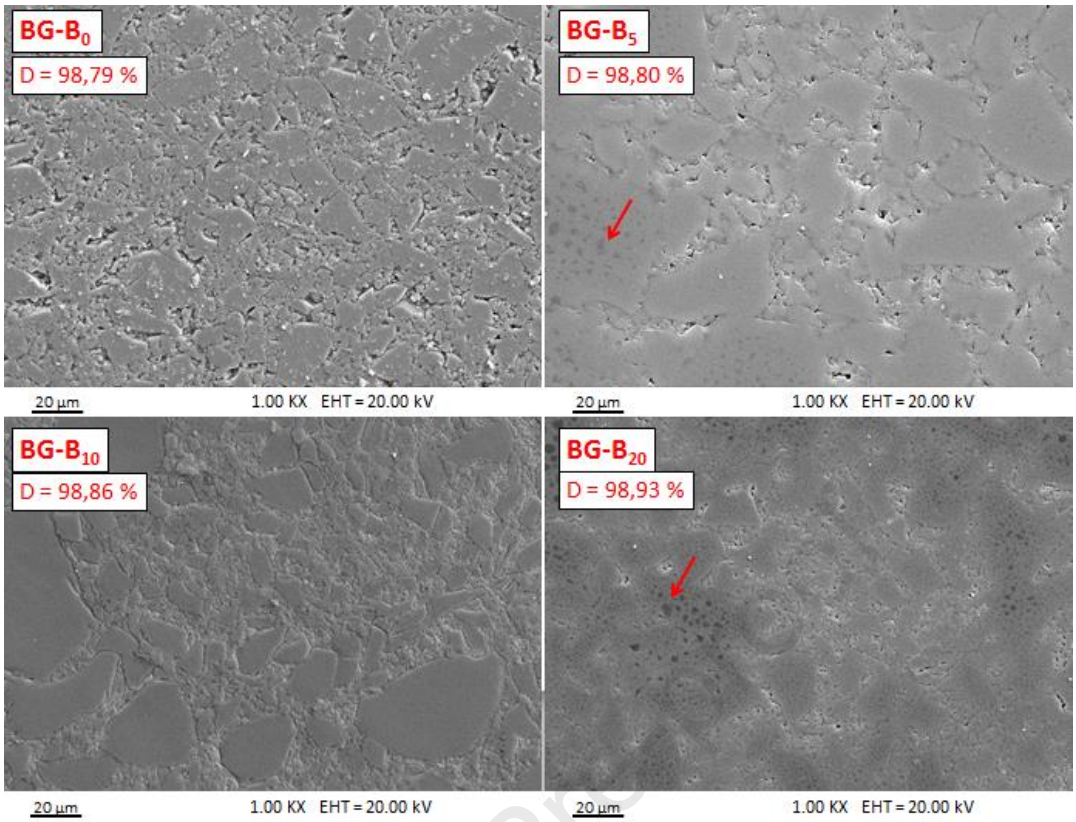
BG-B0
D = 98,79 %
BG-B5
D = 98,80 %
20 µm
1.00 KX EHT = 20.00 kV
20 µm
1.00 KX EHT = 20.00 kV
BG-B10
D = 98,86 %
BG-B20
D = 98,93 %
20 µm
1.00 KX EHT = 20.00 kV
20 µm
1.00 KX EHT = 20.00 kV

Fig. 6

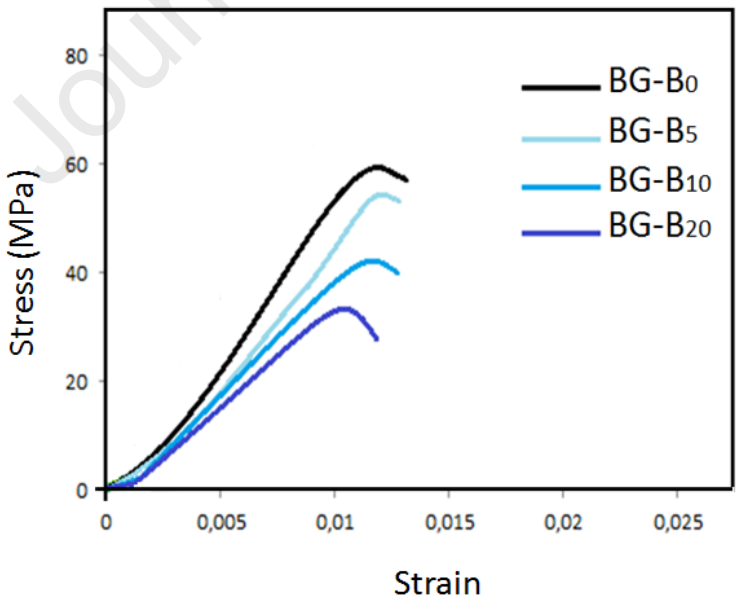
Stress (MPa)
80
60
40
20
0
0
0,005
0,01
0,015
0,02
0,025
Strain
BG-B0
BG-B5
BG-B10
BG-B20

Fig. 7

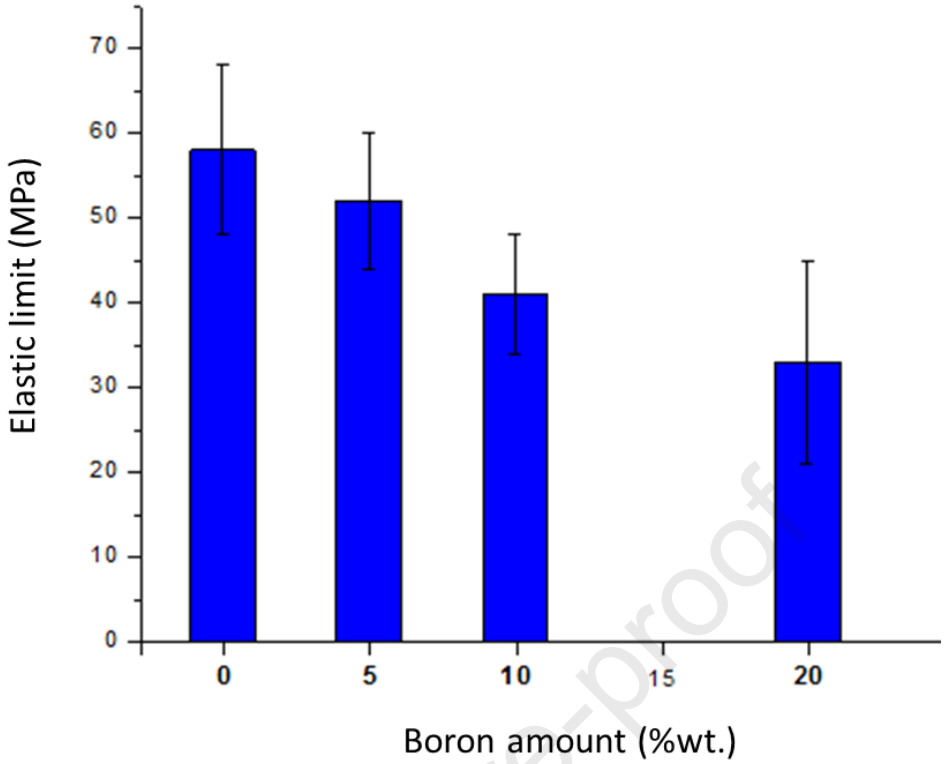
Elastic limit (MPa)
70
60
50
40
30
20
10
0
0
5
10
15
20
Boron amount (%wt.)

Fig. 8

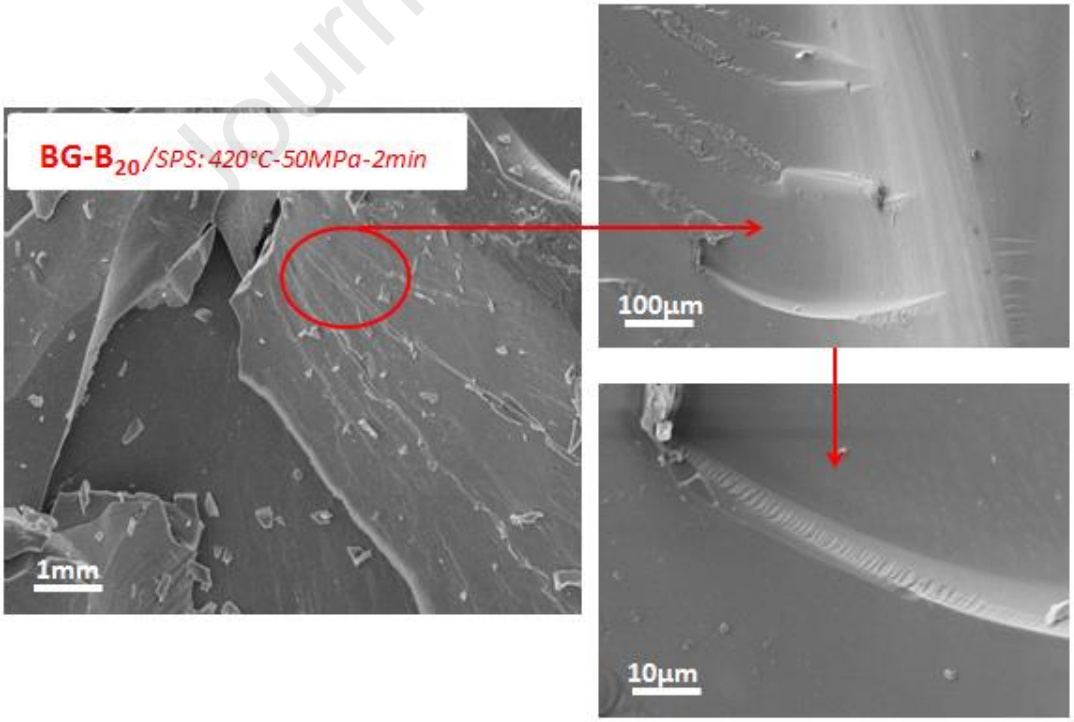
BG-B20/SPS: 420°C-50MPa-2min
1mm
100µm
10µm

Fig .9

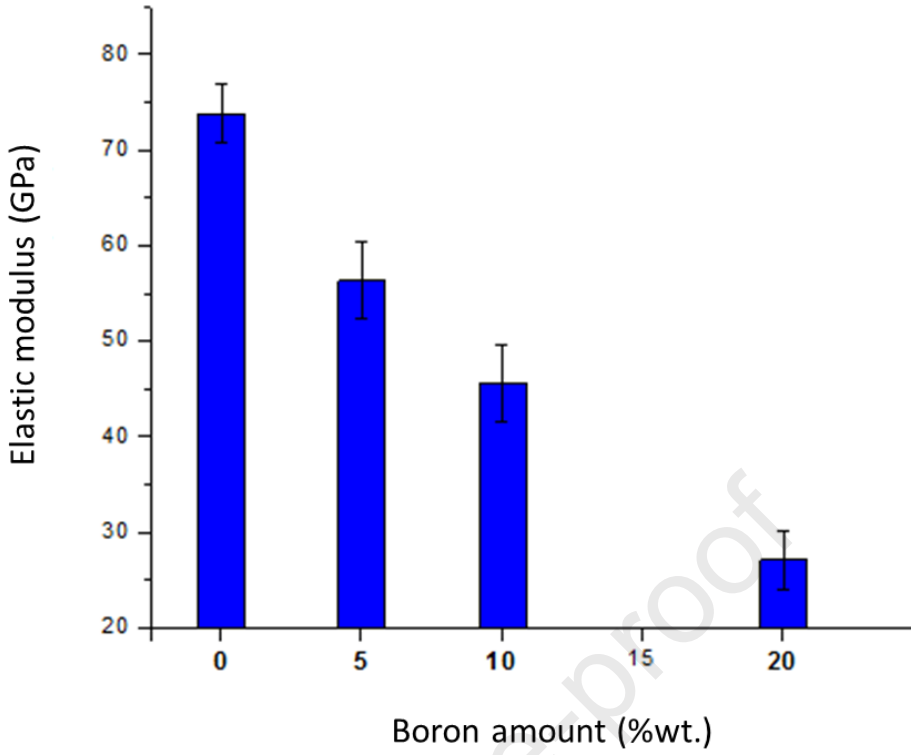
Elastic modulus (GPa)
80
70
60
50
40
30
20
0
5
10
15
20
Boron amount (%wt.)

Fig .10

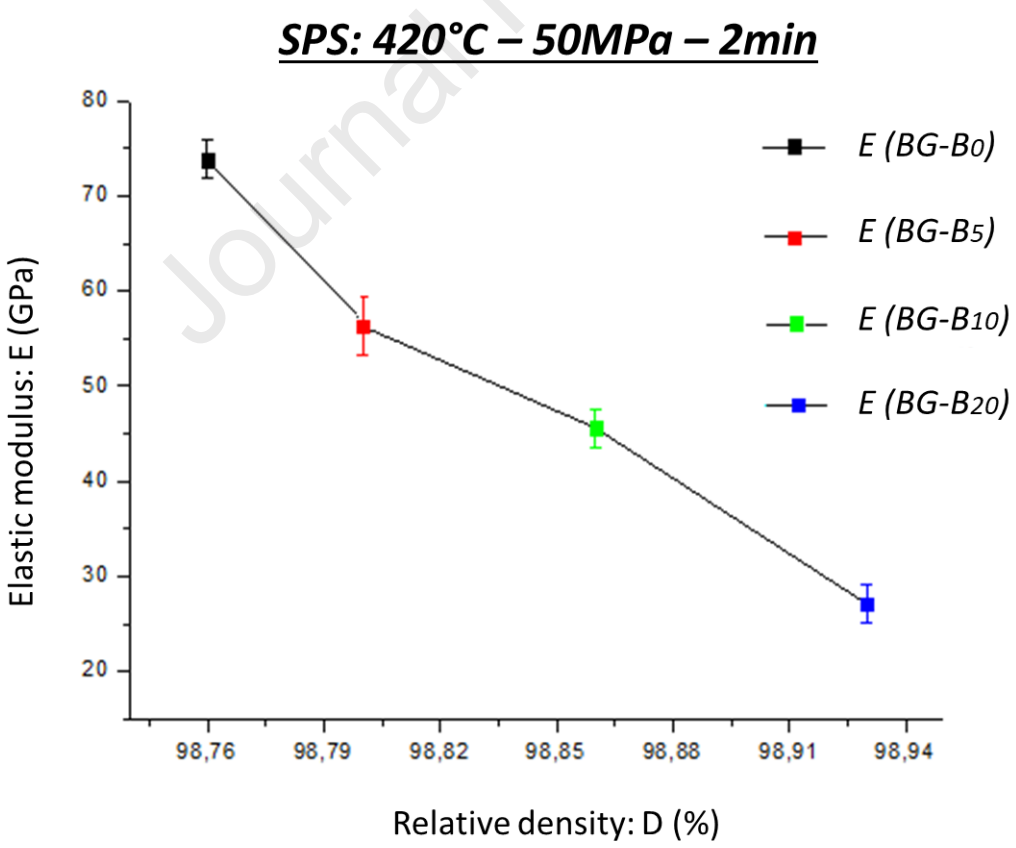
SPS: 420°C – 50MPa – 2min
Elastic modulus: E (GPa)
80
70
60
50
40
30
20
98,76
98,79
98,82
98,85
98,88
98,91
98,94
Relative density: D (%)
E (BG-B0)
E (BG-B5)
E (BG-B10)
E (BG-B20)

Fig. 11

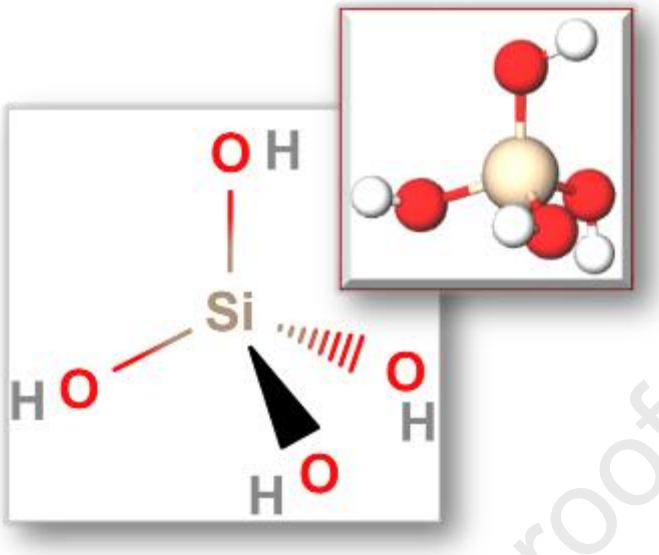

Fig. 12

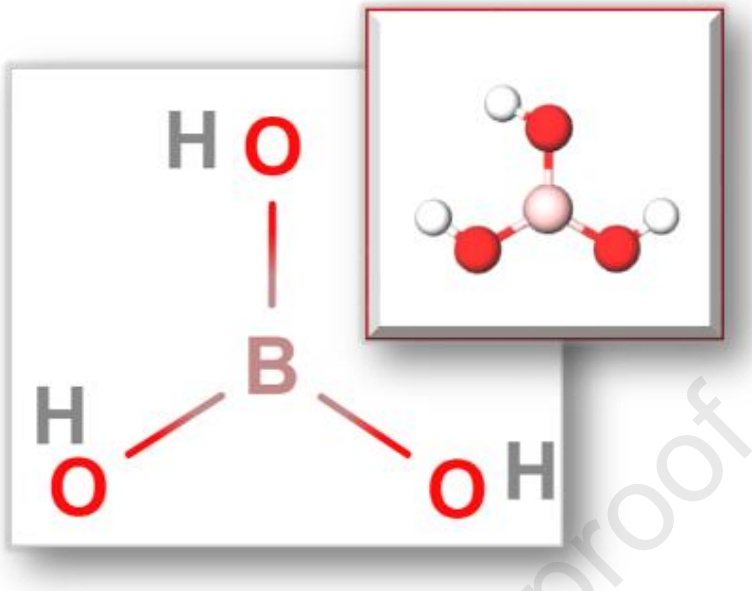

Fig. 13

Table Captions

Table 1: Oxide compositions (in wt.%) of the elaborated glasses.

Table 2: The maximum densification durations and values of synthetized bioactive glasses.

Table 3: The Compressive strength of sintered glass with various quantities of boron.

Table 4: The elastic modulus of the sintered BG-BX bioactive glasses.

Table 1

BG-B_X	SiO_2	CaO	Na_2O	P_2O_5	B_2O_3
BG-B_0	**46**	24	24	6	**0**
BG-B_5	**41**	24	24	6	**5**
BG-B_{10}	**36**	24	24	6	**10**
BG-B_{20}	**26**	24	24	6	**20**

Table 2

BG-B_X	Maximum densification duration (min : s)	Relative density (%)
BG-B_0	08 :58	98,76
BG-B_5	09 :19	98,80
BG-B_{10}	09 :43	98,86
BG-B_{20}	10 : 01	98,93

Table 3

	BG-B_0	BG-B_5	BG-B_{10}	BG-B_{20}
Elastic limit: R_m [MPa] (± 8)	58	52	41	33

Table 4

	BG-B_0	BG-B_5	BG-B_{10}	BG-B_{20}
Elastic modulus: E[GPa](± 3)	73,8	56,3	45,6	27,1

References

[1] E. Gentleman, J.M. Polak, J. Mater. Sci.: Mater. Med. 17 (2006) 1029.
[2] N.Moritz, PK .Vallittu, Bioactive silicate glass in implantable medical devices (2017) Chapter 19.
[3] G. Kaur, V. Kumar, F. Baino, Mater. Sci. Eng. C. 104 (2019) 109895.
[4] L.L. Hench, J. Am. Ceram. Soc. 81 (1998) 1705.
[5] X. Kesse. Thesis University Clermont Auvergne (2019).
[6] F.Z. Mezahi, A.L. Girot, H. Oudadesse, J. Non-Cryst. Solids 361 (2013) 111.
[7] A. Saranti, I. Koutselas, M.A. Karakassides, J. Non-Cryst. Solids 352 (2006) 390.
[8] R.F. Brown, M.N. Rahaman, A. B. Dwilewicz, J. Biomed Mater. Res. 88 (2009) 392.
[9] G. Kaur, O. P. Pandey, K. Singh, J. Biomed. Mater. Res. Part A 102 (2014) 254.
[10] F. J. Torres and J. Alarcon, J. Non-Cryst. Solids 34 (2004) 45.
[11] A. L. Girot, F. Z. Mezahi, M. Mami, J. Non-Crsyt. Solids 357 (2011) 3322.
[12] P. A. Gunatillake, R. Adhikari, Eur. Cells Mater. 5 (2003) 1.
[13] J. R. Jones, A. R. Boccaccini, Cellular Ceramics (2006) 547.
[14] P.K. Vallittu, J. Mater. Sci. 52 (2017) 8772.
[15] E. Boccardi, F. E. Ciraldo, A. R. Boccaccini, MRS Bull. 42 (2017) 226.
[16] M.Y. Choa, D. W. Leeb, I.S Kima, Ceram. Int. 45 (2019) 6702.
[17] C. Feng, K. Zhang, R. He, J. Adv. Ceram. 9 (2020) 360.
[18] R. Wetzel, M. Blochberger, F. Schefer, L. Hupa, Sci. Rep. 10 (2020) 15964.
[19] D.C. Clupper, L.L. Hench, J. Non-Cryst. Solids 318 (2003) 43.
[20] L. Lefebvre, J. Chevalier, L. Gremillard, Acta Mater. 55 (2007) 3305.
[21] V.J. Shirtliff, L.L. Hench, J. Mater. Sci. 38 (2003) 4697.
[22] P. Li, F. Zhang, T. Kokubo, J. Mater. Sci. : Mater. Med. 3 (1992) 452.
[23] L. Lefebvre, L. Gremillard, J. Chevalier, Acta Biomater. 4 (2008) 1894.
[24] L. Lefebvre, J. Chevalier, L. Gremillard, MATERIAUX (2006).
[25] A. Mechay, H. E. Feki, F. Schoenstein, Int. J. Adv. Chem. 2 (2014) 80.
[26] S. Grasso, R. Krishna, A. R. Boccaccini, J. Non-Cryst. Solids 362 (2013) 25.
[27] Z. Li, W. Zhu, S. Bi, J. Biomed. Mater. Res. 108 (2020) 1016.
[28] T. Duerig, A. Pelton, Materials Properties Handbook (1994) 1035.
[29] M. Geetha, A. K. Singh, R. Asokamani, Prog. Mater. Sci. 54 (2009) 397.
[30] M. Niinomi, Int. J. Artif. Organs 11 (2008) 105.
[31] A. Gharbi, H. Oudadesse, H. E. Feki, Int. J. Eng. Technol. 5 (2015) 3.
[32] A. Mishra, P. Noppari, C. B. Plédel, J. Appl. Glass. Sci. 11 (2020) 622.
[33] A. Gharbi, H. E. Feki, H. Oudadesse, Korean J. Chem. Eng. 32 (2015) 1.
[34] L.L. Hench, J. Wilson, An Introduction to Bioceramics (1999) 411.
[35] S. Fagerlund,L. Hupa, RSC. Chapter 1 (2016) 1.
[36] AR. Boccaccini, DS. Brauer, L. Hupa, RSC (2016) 442.
[37] S. Grasso, Y. Sakka, G. Maizza, Sci. Technol. Adv. Mater. 10 (2009) 053001.
[38] D. Shekhawat, A. Singh, M. K. Banerjee, Ceram. Int. 47 (2021) 3013.
[39] S. Kanhed, S. Awasthi, S. Goel, Ceram. Int. 43 (2017) 10442.
[40] S. Grasso, C. Hu, B.N. Kim, J. Am. Ceram. Soc. 94 (2011) 1405
[41] O. Bretcanu, X. Chatzistavrou, A. R. Boccaccini, J. Eur. Ceram. Soc. 29 (2009) 3299.
[42] O. Guillon, S. Cao, A. R. Boccaccini, J. Eur. Ceram. Soc. 31 (2011) 999.
[43] J. Massera, S. Fagerlund, L. Hupa, J. Am. Ceram. Soc. 95 (2012) 607.
[44] F. Baino, E. Fiume, Mater. Lett. 224 (2018) 54.
[45] O. Peitl, E.D. Zanotto, L.L. Hench, J. Non-Cryst. Solids, 292 (2001) 115.
[46] H. Arstila, L. Hupa, K. Karlson, Eur. J. Glass Sci. Technol. 48 (2007) 196.
[47] L. Ramond, G. B. Granger, A. Addad, J. Am. Ceram. Soc. 94 (2011) 2926.
[48] W. Xia, J. Chang, Mater. Lett. 61 (2007) 3251.
[49] S. Grangeon, F. Claret, Y. Linard, Acta. Crystallogr. Sect. B Struct. Sci. Cryst. Eng. Mater. 69 (2013) 465.
[50] X. Bui, T. Dang, Process. Appl. Ceram. 13 (2019) 98.
[51] Y.-F. Goh, A.Z. Alshemary, M. Akram, Int. J. Appl. Glas. Sci. 5 (2014) 255.
[52] A. Meiszterics, L. Rosta, H. Peterlik, J. Phys. Chem A.114 (2010) 10403.
[53] P. Kongsuwan, G. Brandal, Y.L. Yao, J. Manuf. Sci. Eng. 137 (2015) 1.

[54] L. Deilmann, O. Winter, B. Cerrutti, J. Mater. Chem. B 8 (2020) 1456.
[55] M.P. Staiger, A.M. Pietak, J. Huadmai, Biomaterials 27 (2006) 1728.
[56] X. Li, G. Lu, Z. Zhang, J. Alloys Compd. 647 (2015) 917.
[57] L. Desogus, A. Cuccu, S. Montinaro, J. Eur. Ceram. Soc. 35 (2015) 4277.
[58] H.B. Guo, X. Miao, Y. Chen, Mater. Lett. 58 (2004) 304.
[59] Q.Z. Chen , J.L. Xu, L.G. Yu, Mater.Sci.Eng.C 32 (2012) 494.
[60] F. Baino, E. Fiume, Biomed. Glasses 6 (2020) 50.
[61] C. Viney, Biomaterials Science 3rd ed. (2013) 9.
[62] N.A.P. van Gestel, F. Gabriels, B. van Rietbergen, Bioactive Glasses 2nd ed. (2018) 87.
[63] V.K. Marghussian, A. S-M. Mesgar, Ceram. Int. 26 (2000) 415.
[64] H.Yli-Urpo, L.V.J. Lassil, P.K. Vallittu. Dent. Mater. J. 21 (2005) 201.
[65] E.I. Kamitsos, A.P. Patsis, M.A. Karakassides, J. Non-Cryst. Solids 126 (1990) 52.
[66] O. Prokopiev, I. Sevostianov, Mater.Sci. Eng.A 431 (2006) 218.
[67] M.H. Elahinia, M. Hashemi, M. Tabesh, Prog. Mater. Sci. 57 (2012) 911.
[68] T. Duerig, A. Pelton, D. Stöckel, Mater. Sci. Eng. A 273 (1999) 149.
[69] T. Aydoğmuş, Ş. Bor, J. Mech. Behav. Biomed. Mater. 15 (2012) 59
[70] D. Mondal, S. J. Dixon, K. Mequanint, J. Mech. Behav. Biomed. Mater. 75 (2017) 180.
[71] M.Abderrahmen, Thèse de l'Université Paris XIII Sorbonne Paris cité (2014).
[72] Y.H.Yun, P.J.Bray, J. Non-Cryst. Solids 27 (1978) 363.
[73] W.J.Dell, P.J.Bray, S.Z.Xiao, J. Non-Cryst. Solids 58 (1983) 1.
[74] B.Łagowska, I.Wacławska,M.Sitarz, J. Mol. Struct. 1171 (2018) 110.
[75] B. Raguenet, Thèse University of Montpellier II, Sciences et Techniques du Languedoc, (2011).
[76] R. Sergi, D. Bellucci, V. Cannillo, Coatings 10 (2020) 757.

Highlights

- The bioactive glasses powders are elaborated according to the quaternary system: SiO_2-Na_2O-CaO-P_2O_5-x B_2O_3 system (0 <x< 20 wt.%); have been consolidated using Spark Plasma Sintering (SPS).

- It was possible to achieve fully dense and vitreous borated glasses at 420 °C.

- The physic-chemical and mechanical properties of these materials were investigated in this study to prove that these glasses able to be a promising candidate for bone implant.

Declaration of interests

☒ The authors declare that they have no known competing financial interests or personal relationships that could have appeared to influence the work reported in this paper.

☐The authors declare the following financial interests/personal relationships which may be considered as potential competing interests: